AUGUST 2002
VOL. 13, NO. 2

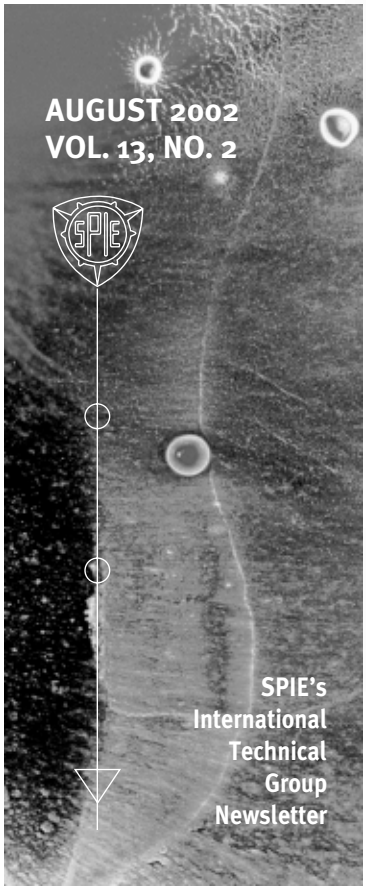

Optics in Information Systems

Optically-interconnected computing at Heriot-Watt University

The Department of Physics at Heriot-Watt University, Edinburgh, has been working in the fields of optical computing and optical interconnects for the last twenty years. This article will look at two of the projects recently completed by the current Optically Interconnected Computing (OIC) Group.

The first of these is the AMOS (Analysis and Modelling of Optoelectronic Systems) project which is an investigation of the impact of a highly-interconnected, high-bandwidth interconnect on a commodity-PC-based cluster. We constructed a set of models to describe an optical highway consisting of a number of nodes interconnected by a free-space optical system.[1] Each node consisted of a PC and a smart-pixel array (SPA) providing the optoelectronic interface and, potentially, other functionality such as caching or low-level network operations (see Figure 1). The Institute of Informatics at The University of Leeds then used this description of the hardware in simulations of a number of algorithms. The models used for the AMOS project allow for a large degree of freedom in designing the optical system, choosing the PC architecture, and designing the algorithm to run on it.

It was clear that the relatively low bandwidth of the PC I/O bus would limit any system connected to it. It was found that the optical highway can enhance the performance of a PC cluster in two ways. First, the massive interconnectivity can be used to create large, completely-connected (or near-completely-connected) networks. This high connectivity reduces the latency of messages as fewer routing decisions are required and fewer network links are travelled. Second, some functionality—such as a random stealing load balancing algorithm—can be implemented on the SPA layer. Here, tasks are stored on the SPA

Continues on page 9.

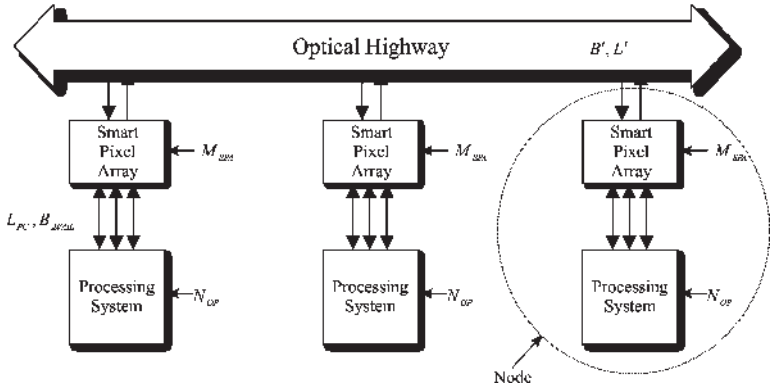

Figure 1. Schematic of the optical highway model used in the AMOS project. This shows the highest level of abstraction. Each parameter is obtained from lower level models of the system.

First of two special issues on:
Optical Computing 2002

Edited by **Ken Hsu,** Institute of Electro-Optical Engineering National Chiao Tung University

Newsletter now available on-line

Technical Group members may now receive the Optics and Information Systems Newsletter electronically. An e-mail has been sent to all group members with details of the web location for this issue, and asking members to choose between the electronic and printed version for future issues. If you are a member and have not yet received this message, then SPIE does not have your correct e-mail address.

To receive future issues electronically, please send your e-mail address to:
`spie-membership@spie.org`
with the word `OIS` in the subject line of the message and the words `electronic version` in the body of the message.

If you would like to continue to receive the newsletter in the printed format, but want to send your correct e-mail address for our database, please include the words `print version preferred` in the body of your message.

Detection of 3D object position using a lens array and joint-transform correlator

Over the past few decades, considerable progress has been achieved in image recognition techniques using optical correlators in the two-dimensional (2D) plane. This progress has included the development of numerous techniques for scale, rotation, and shift-invariant detection. Recently, however, a new type of optical correlator capable of performing a correlation operation in three-dimensional (3D) space has attracted attention. The 3D correlator extends the region of the correlation operation from the 2D plane to a 3D space while retaining the advantages of the conventional 2D correlator. Among several proposed methods,[1-4] the lens-array-based technique is advantageous because it allows for the capture of many object perspectives simultaneously. This results in a relatively small digital processing load. We have been developing such a 3D-image-recognition technique.

Figure 1 shows the setup used: reference and signal objects are imaged by the lens array and the resulting elemental images are captured by charge-coupled devices (CCDs). Each elemental image contains information concerning the corresponding perspective according to the relative position of each lens to the object. Our method involves some digital processing of the elemental images, followed by use of a joint-transform correlator (JTC) between the corresponding elemental images of the reference and signal objects. The 3D position of the signal object is obtained by locating elemental image pairs in which perspectives can be made the same by resizing the elemental images with respect to their centers. Such pairs satisfy two conditions: the elemental images should have the same perspective of the objects, and the positions of these perspectives should only be dependent on the distance of the object from the lens array (and, therefore, independent of the lateral position of the elemental lens).

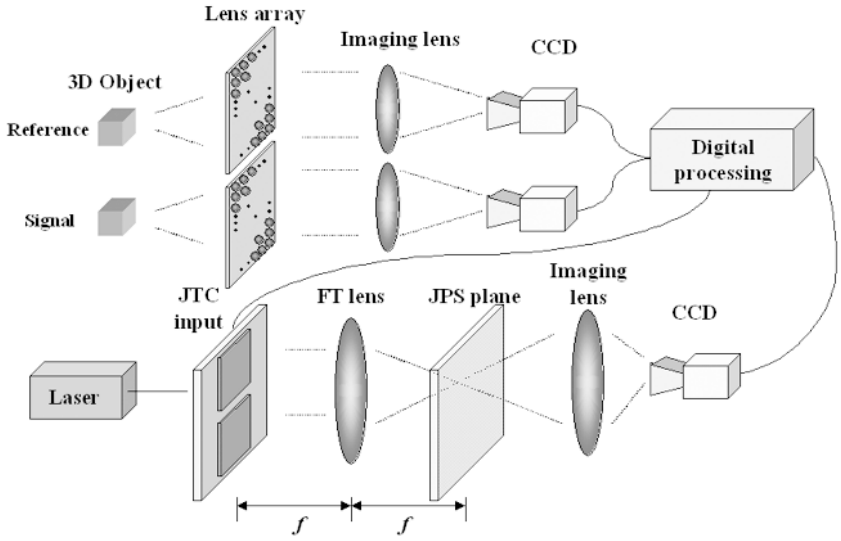

Figure 1. Three-dimensional correlator using a lens array.

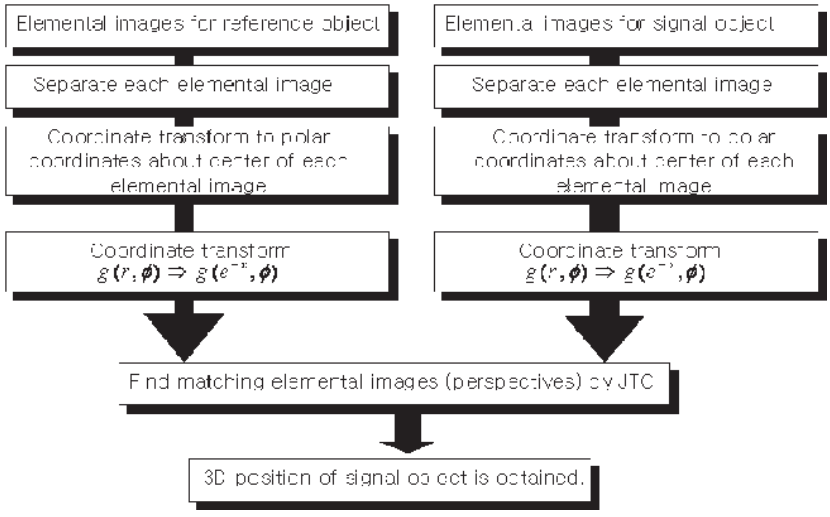

Figure 2. Flow-chart of the proposed 3-D correlation technique.

The perspective captured by each elemental lens depends on the angle at which it views the object. This is determined by the ratio of the distance of the object from the lens array and the difference in lateral position between the center of the object and that of the elemental lens. The position of the perspective in the elemental image also depends on the ratio of the object distance (from the lens) and the difference between the lateral position of the object and its corresponding elemental lens. The size of the perspective only depends on the object distance.

Assuming that the signal object and the reference object are identical—with no lateral shift—but are positioned at different distances from the lens array, the elemental image pairs captured at the same non-zero angles cannot be made the same by adjusting their size while fixing their centers. This is despite the fact that they represent the same perspective of the objects. This is because the positions of the perspectives with respect to the centers of the corresponding elemental images are the same, while the sizes of the perspectives are different. Only the elemental image pair at angle zero can be made the same by adjusting its size, since the lateral positions of the corresponding elemental lens with respect to the objects are zeros. Thus the condition related to the perspective position is satisfied.

When the signal object shifts laterally, the elemental lens at angle zero changes. The difference in lateral position between the elemental lenses at angle zero can be approximated as the lateral shift of the object. At the same time, this limits the maximum error to a value below the half spacing between adjacent elemental lenses. Since the longitudinal position of the object can be obtained by the size difference between the same perspectives, the 3D position of the signal object with respect to the reference object can be obtained by detecting, scale-invariantly, the elemental image pair with angle zero views.

For scale-invariant detection, we apply the Mellin transform. As this provides information about the size of the input images, the longitudinal position of the signal object with respect to the reference object can be found. Before performing the Mellin transform, however, we change the

Continues on page 9.

All-optical pulse generators for optical computing

The promise and power of an optical computer is that it can do things that can't be done by a digital computer. But a digital serial machine can emulate almost anything, and in the past there have been repeated instances where supposedly intractable problems have yielded to the rising tide of digital processing power, memory and speed. Can we expect optical computers to ever accomplish anything that cannot be done by a now—or future—digital computer? It is a good question. There are good answers, some of which I will describe here, of one-step parallel computational methods for optical pulse networks.

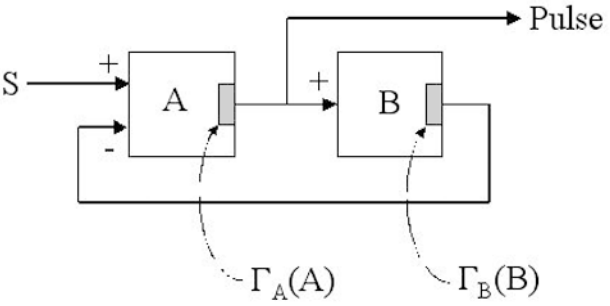

Figure 1. An excitatory-inhibitory pair.

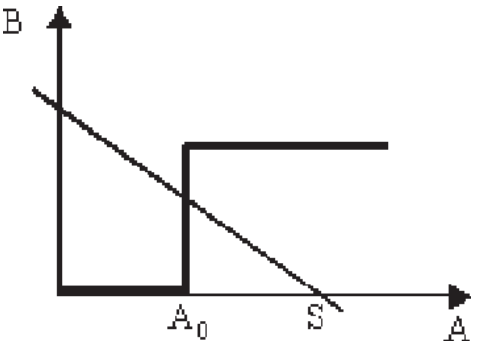

Figure 2. Nullcline diagram of a pulse generator.

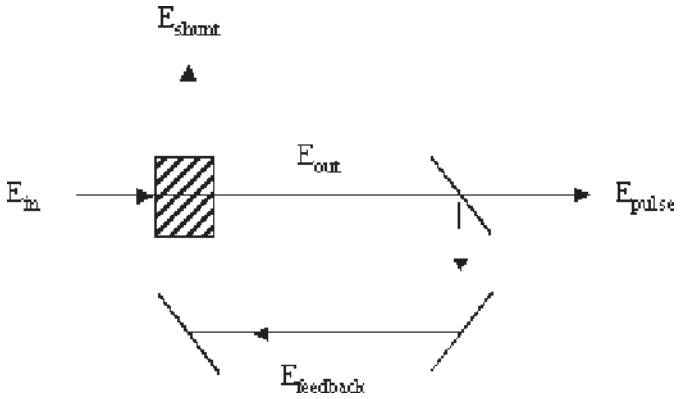

Figure 3. A photorefractive pulse generator.

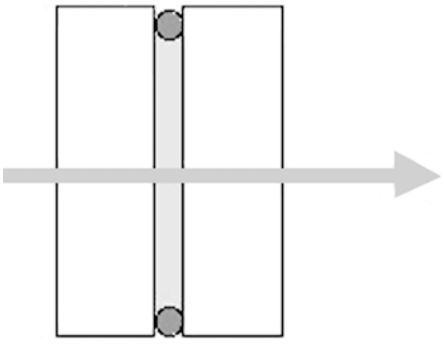

Figure 4. A nonlinear F-P pulse generator.

Pulse generator mechanisms

A general model for generating pulse waveforms consists of two nonlinear signal response elements coupled as an excitatory-inhibitory pair (see Figure 1). If $G_A = Step(A\text{-}A_0)$ and $G_B = kB$ (see Figure 2) then when A rises above A_0 the inhibitory element's internal activity B receives a step increase. This in turn abruptly decreases A to below the threshold A_0. The step function is first triggered and then almost immediately reset to zero. It is a simple integrate-and-fire generator.

Optical pulse generators

An elegant pulse generator by Wang[1] uses a mixed excitatory-inhibitory pair of elements with biased, subtractive, inhibition as well as shunting inhibition for both elements. It consists of a photorefractive cube whose induced grating is the result of the interaction between the incident laser beam and a part of the output beam that is fed back to the cube (see Figure 3). As soon as the grating is formed, it shunts away the feedback beam. This destroys the induced grating, which lets the feedback beam return, and the cycle repeats.

Another pulse generator by Wang (see Figure 4) uses a nonlinear Fabry-Perot etalon. Here, the liquid crystal itself provides multiple competitive nonlinearities. Pulse rates above 100 Hz have been achieved with this system (see Figure 5).

One-step information processing

What can one compute in a single step? We are accustomed to thinking in terms of serial architectures where each step accomplishes only a small part of the computation. But parallelism is the rule in neural systems, so we can look to them for some ideas and basic tools on how to perform an entire computation in a single step. A completely parallel input consists of a field of pulses within a single short time interval. The order of arrival of the pulses carries information as a time-of-arrival or rank-order code. Thorpe et. al[2,3] shows that many complex neural algorithms can be implemented by these codes.

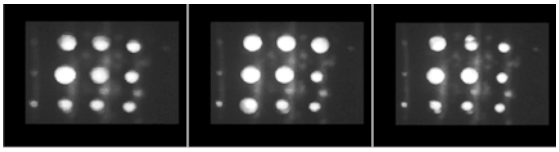

Figure 5. Three by three array: pulse generator output sequence.

Consider a group of N neurons, K of which have fired within a time window T. If we use the average firing rate, the only information we get is that K out of $N+1$ possible counts occurred in the time interval. The information capacity available is $log_2(N+1)$ bits. This is one of the lowest information-bearing coding schemes. An interspike time-interval code gives the opposite extreme. For a time resolution D there are $V=T/D$ possible values per channel. For each of those we can choose V values of the next channel, and so with N channels we have V^N possible choices, and an information capacity of $N*log_2V$ bits. Finally, the rank-order coding method allows $N!$ possible states and has an information capacity of $log_2N!$ bits.

An integrate-and-fire pulse generator has an increasing firing rate with increasing input signal strength. The neurons that fire first are those with the strongest input signals. Since their inputs can be tuned by the shape of their receptive fields to a variety of geometrical features (contrast, orientation, and lines, for example), the first pulses to arrive are those from the most prominent features and important parts of the image. Thorpe's work shows that most of the information content of images is contained in the first 1%-2% of the pulses.

Summary

Optics allows the design of non-digital, massively-parallel architectures, but its very virtue (linear superposition) prevents it from forming logical elements. The design of all-optical pulse generators provides this additional capability. Review

Continues on page 9.

Polarity-controlled growth of III-nitrides and their potential applications in optoelectronic devices

Semiconductor-based optoelectronic devices have formed the basis for optical computing.[1] However, applications have been limited by the lack of materials that work efficiently in the green-to-ultraviolet regions. In last decade, III-nitrides have emerged as the most promising candidates for short-wavelength optoelectronic devices. Much progress has been made in III-nitride growth, but the technology is still not sufficiently developed to grow AlGaN/(In)GaN multiple quantum well structures (MQWs) for ultrahigh performance devices such as VCSELs or intersubband-transition quantum structures.

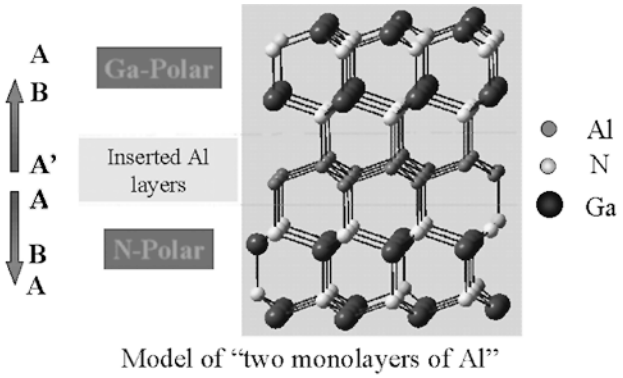

Figure 1. GaN-polarity conversion from N to Ga polarity by insertion of two monolayers of Al.

One of the main characteristics of III-nitrides is polarity, which is of major importance both in the epilayer growth and device fabrication.[2] Many factors have been reported to affect epilayer polarity: these include the growth method, substrate nitridation, buffer-layer materials, buffer-layer growth temperature, growth rate, etc.. To date, films grown with Ga polarity show superior properties to those grown with that of N. A high-temperature-grown AlN layer, or In irradiation on the growing surface, have been reported to reverse N polarity to that of Ga. More recently, it was found that, during AlGaN/GaN growth, the epilayer polarity can swing from that of Ga to N and back again frequently depending on the growth temperature. However the related mechanisms are not yet clear. To grow high-quality MQWs and supperlattices for sophisticated optoelectronic devices, it is crucial to clarify these polarity selection processes and inversion mechanisms.

We have systematically investigated the polarity selection and conversion process of GaN grown using moecular beam epitacy (MBE). Based on this work, we have established a framework for the understanding, control and manipulation of GaN polarities. We have also considered the potential application of polarity-controlled growth in optoelectronic devices. (Details of the MBE growth process and the characterization of polarities of GaN films by coaxial impact collision ion scattering spectroscopy (CAICISS) have been reported elsewhere.[3,4])

First, sapphire-substrate surface termination was investigated by in-situ CAICISS during the thermal cleaning process (up to 850˚C in ultra-high vacuum). It was revealed that the sapphire (0001) surface became Al-terminated when the substrate temperature was raised to 700˚C, and Al-rich sapphire surface could be obtained after thermal cleaning treatment at 850˚C for 30min.

For a GaN epilayer grown on a non-nitrided sapphire substrate, well-defined Ga polarity was shown. For a film grown on extensively-nitridated sapphire substrate, N polarity was not pure: there was a 5% Ga-polarity inversion domain. These results provided a framework to enable us to understand the polarity of the GaN epilayer. Both thermal cleaning and nitridation must be taken into account.

Ga polarity is preferred for GaN grown on a non-polar sapphire substrate after thermal cleaning, which can make it Al-rich. Is it possible to reverse GaN polarity by introducing an ultra-thin Al layer? The answer to this question is technologically important, both for polarity manipulation and the elimination of the polarity inversion domain. Results show that, by depositing two monolayers (ML) of Al on GaN with N polarity during epitaxy, a Ga-polarity epilayer could be obtained. The related mechanism is schematically shown in Figure 1. Geometrically, it is identical to the bonding of two N-polarity layers by two ML of Al. Extensive work has been done on the polarity-conversion process via an Al insertion layer.[3,4]

GaN polarity selection on an AlN intermediate layer was also investigated, with emphasis on AlN surface stoichiometry. Basically, high-temperature AlN intermediate layers of about 20nm thick were grown on N-polarity GaN in N-rich or Al-rich conditions.[4] The results showed that AlN intermediate layers grown in N-rich conditions did reverse the N to Ga polarity, while those grown in Al-rich conditions could also reverse the GaN polarity. Furthermore, experiments showed that excess Al was crucial for the realization of GaN polarity conversion, consistent with polarity conversion by Al insertion layers.[3]

The potential applications of polarity control are not only for the growth of unipolar epilayers and the elimination of mixed polarities, but also for the the minimization of the negative effects of the intrinsic, huge, spontaneous, polarization and pyroelectric fields that exist at the hetero-interfaces of grown polarity-inverted structures.

One positive use of mixed polarity is that the inversion-domain boundary has been reported as an optically-active center for carriers.[5] This kind of inversed domain is promising as a means of enhancing the performance of ultraviolet LEDs by using mixed-polarity GaN as the active layer.

Homo-epitaxy of GaN on a hydride-vapor-phase-epitaxy- (HVPE-) grown template is attractive because of the expected high quality and simple structure of the device. However, Ohmic contact to the N polarity surface has proved difficult. By applying polarity-controlled growth, we can get a GaN substrate with Ga polarity both on the front and back surfaces: favorable for device processing. The polarity-inversion structure sandwiched with the ultra-thin Al layer shown in Figure 1 should prove useful in the integration of electronic and optoelectronic devices.

A. Yoshikawa* and K. Xu
*Center for Frontier Electronics
and Photonics
Department of Electronics
and Mechanical Engineering
Chiba University
1-33 Yayoi-cho, Inage-ku
Chiba 263-8522, Japan
Tel: +81 43 290-3990
Fax: +81 43 290-3991
E-mail: yoshi@cute.te.chiba-u.ac.jp

References

1. N. Iizuka, K. Kaneko, N. Suzuki, T. Asano, S. Noda, and O. Wada, *Ultrafast intersubband relaxation (150 fs) in AlGaN/GaN multiple quantum wells*, **Appl. Phys. Lett. 77** (5), pp. 648-650, 2000.
2. F. Bernardini, V. Fiorentini, and D. Vanderbilt, *Spontaneous polarization and piezoelectric constants of III-V nitrides*, **Phys. Rev. B 56** (16), p. R10024, 1997.
3. K. Xu, N. Yano, A. W. Jia, A. Yoshikawa, and K. Takahashi, *Kinetic process in polarity selection of GaN grown by RF-MBE*, **Phys. Stat. Sol. B 188**, pp. 523-527, 2001.
4. K. Xu, N. Yano, A. W. Jia, K. Takahashi, and A. Yoshikawa, *Polarity Control of GaN Grown on Sapphire Substrate by RF-MBE*, **J. Crystal Growth 237-239 P2,** pp. 1003-1007, 2002.
5. P. J. Schuck, M. D. Mason, R. D. Grober, O. Ambacher, A. P. Lima, C. Miskys, R. Dimitrov, and M. Stutzmann, *Spatially resolved photoluminescence of inversion domain boundaries in GaN-based lateral polarity heterostructures*, **Appl. Phys. Lett. 79** (7), pp. 952-954, 2001.

Femtosecond optical information processing via Fourier optics

In the Ultrafast Optics and Optical Fiber Communications Laboratory at Purdue University, our research focuses on femtosecond Fourier-optical techniques for processing ultra-high-speed, broadband, optical signals. The application of Fourier-optical ideas in the ultrafast time domain— originally explored in the context of spatial image processing—is extremely fruitful and provides rich possibilities for high-speed optical signal processing. Our research aims to develop new and sophisticated signal manipulation techniques within the context of ultrafast optics, and to apply these techniques to problems in ultra-high-speed communications.

In the following, I briefly touch on some of the work in my laboratory on ultrafast optical techniques for synthesizing, transmitting, processing, and receiving optical waveforms and bit sequences with features in the femtosecond regime. An important theme is the conversion between time, frequency, and space domains via time-domain Fourier-optical approaches, emphasizing realizations compatible with the requirements (wavelength, power, speed) of real-world photonic applications.

For some time my group has been actively pursuing linear, ultrafast, optical-pulse-shaping techniques, which allow programmable synthesis of nearly arbitrary ultrafast optical waveforms via wavelength-by-wavelength control of the complex optical spectrum. This technology is now widely employed in ultrafast optical science, particularly for research on coherent control of quantum mechanical motions. Here I discuss pulse shaping from the perspective of applications in linear and nonlinear photonics. Examples of our research are introduced in the following paragraphs.

- We have applied Fourier-transform femtosecond pulse shaping[1,2] as a spectral phase equalizer for programmable fiber dispersion compensation. This enabled us to demonstrate distortion-free transmission of pulses as short as 400fs over 10km fiber spans, despite the fact that dispersion broadens these pulses by over 1000 times prior to compensation.[3,4] We also applied pulse shaping to simple experiments with ultrashort-pulse optical code-division multiple-access (O-CDMA) communications, resulting in suppression of multi-access interference for error-free operation.[5] Other groups have applied our pulse-shaping geometry in WDM, resulting in, among other things, commercial products permitting wavelength-by-wavelength gain equalization and switching.

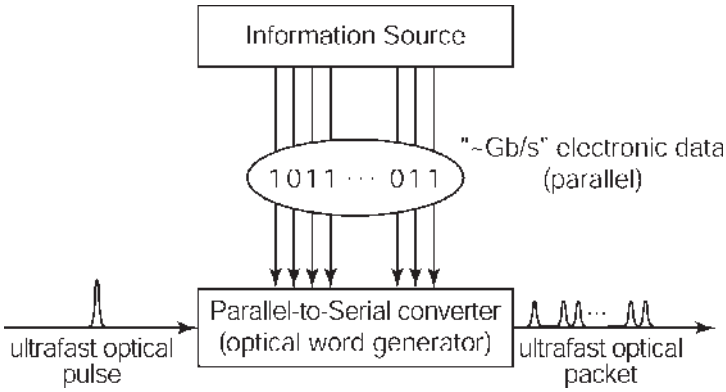

Figure 1. Ultrafast optical parallel-to-serial converter concept.

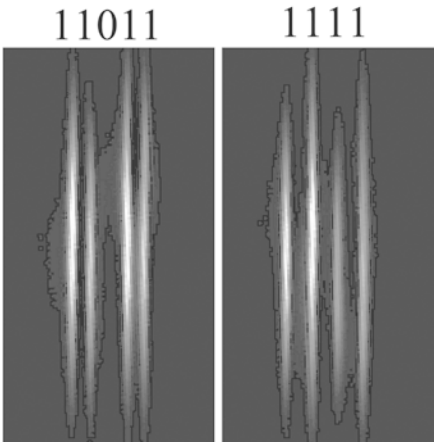

Figure 2. Time-to-space converter images of ultrafast optical pulse sequences in the lightwave communications band. The pulse spacing for the sequence on the left was 2.2ps.

- Recently, we demonstrated the operation of a new, direct space-to-time (DST) pulse shaper, applicable to an ultrafast optical parallel-to-serial converter concept. This could potentially offer operation at multi-GHz frame rates (see Figure 1). Our apparatus generates a serial output in the ultrafast time domain that is a directly-scaled version of an input spatial pattern. In the future we hope to modify the input spatial patterns with sub-nanosecond frame times using optoelectronic modulator arrays. The result wil be an optical word generator, reprogrammable at these high rates. We have implemented versions of the DST pulse shaper in both bulk optics[6] and integrated-optical arrayed-waveguide-grating technology.[7] Interestingly, the DST pulse-shaper geometry functions as a new type of generalized spectrometer with a user-definable, and potentially highly structured, spectrometer response function.

- We have also obtained new signal-processing functionalities by combining pulse shaping with nonlinear optics. Examples include: a spectral, nonlinear-optical time-to-space (serial-to-parallel) converter[8-10] for ultrafast demultiplexing and waveform measurement; and a novel spectral correlator for ultrafast waveform recognition in O-CDMA receivers based on narrow-band second harmonic generation.[11,12] Figure 2 shows spatial images of ultrafast optical bit sequences at 1.56μm wavelength produced by our spectral nonlinear-optical time-to-space converter.[10] To our knowledge, this is the first demonstration of time-to-space converter operation in the lightwave communications band. Both our time-to-space and spectral correlators have already demonstrated nonlinear-optical conversion efficiencies sufficient to support real-time operation without signal averaging, with high signal-to-noise available directly at the repetition rate of our laser. These are important steps towards practical application of these novel, Fourier-optics-inspired technologies for ultrafast and broadband optical signal processing.

A. M. Weiner
School of Electrical and Computer Engineering
Purdue University
West Lafayette, IN 47907-1285
Tel: (765) 494-5574
Fax: (765) 494-6951
E-mail: amw@ecn.purdue.edu
http://dynamo.ecn.purdue.edu/~amw

References

1. A. M. Weiner, *Femtosecond optical pulse shaping and processing*, **Prog. Quantum Electron. 19,** p. 161, 1995.
2. A. M. Weiner, *Femtosecond pulse shaping using spatial light modulators*, **Rev. Sci. Instr. 71,** p. 1929, 2000.
3. C.-C. Chang, H. P. Sardesai, and A. M. Weiner, *Dispersion-free fiber transmission for femtosecond pulses using a dispersion-compensating fiber and a programmable pulse shaper*, **Opt. Lett. 23,** p. 283, 1998.
4. S. Shen and A. M. Weiner, *Complete Dispersion Compensation for 400-fs Pulse Transmission over 10-km Fiber Link Using Dispersion Compensating Fiber and Spectral Phase Equalizer*, **IEEE**

Continues on page 11.

A fiber Bragg grating senses underwater sound

Using an optical fiber to sense acoustic waves in water has several advantages. First, the low propagation loss of fiber, especially in the wavelength range around 1.5mm, allows us to monitor the signal from a distance. Second, the optical fiber transmission line is inherently immune to electromagnetic interference. Third, many kinds of sensing and/or controlling signals can be transmitted through a fiber, and power can be supplied through the same fiber in some cases. In addition, the sensitivity and dynamic range of the fiber acoustic sensor in water are excellent.

When an ordinary optical fiber is used as the sensing element, detection is usually based on an optical phase shift produced under the influence of an acoustic field: the dynamic pressure. This is exploited in the ocean-based hydrophone array system.[1]

However, fiber Bragg gratings (FBGs) are now the star players in the field of optical fiber sensors, and have been successfully used to detect sound in water.[2,3] Under the influence of sound pressure, the FBG modulates—either in reflection or transmission—the intensity of narrow-spectrum light incident upon it. The characteristic feature of the FBG hydrophone based on intensity-modulation is its simplicity. The phase shift in the lead fiber of the sensor, sensitive to external disturbance, does not influence sensor operation unless some of the light power leaks out (because of the physical deformation of the fiber such as bending).

Figure 1 shows a prototype of the FBG hydrophone head that we made. An FBG is embedded in silicone rubber. One side of the FBG fiber is cut at an angle of 8° in order to reduce the back reflection from the end facet, and the other side is attached to an FC/APC optical connector. To use the FBG hydrophone, narrow-spectrum light (such as a laser beam) must be supplied via an optical circulator or fiber coupler: the circulator is preferable because of its higher performance. The wavelength of the light should be tuned to the slope of the FBG reflection-spectrum curve, on either the longer or shorter wavelength side.

When the hydrophone is placed in water where an acoustic field is present, the light reflected from the hydrophone is intensity-modulated by the sound pressure applied to the FBG. The detection of the light with a photodiode gives us a signal that is directly proportional to the acoustic field in the water: from the resulting temporal waveform, the amplitude and phase of the field can easily be measured after the necessary calibration.

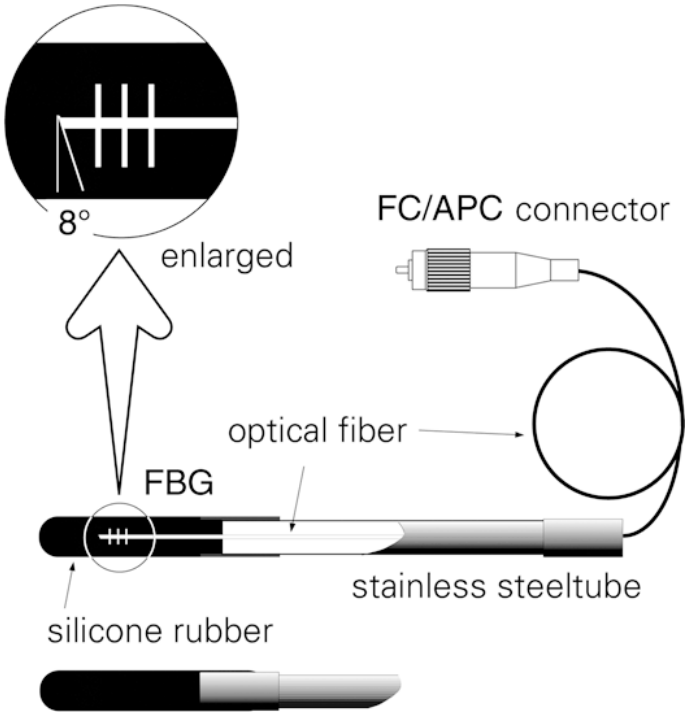

Figure 1. FBG hydrophone head.

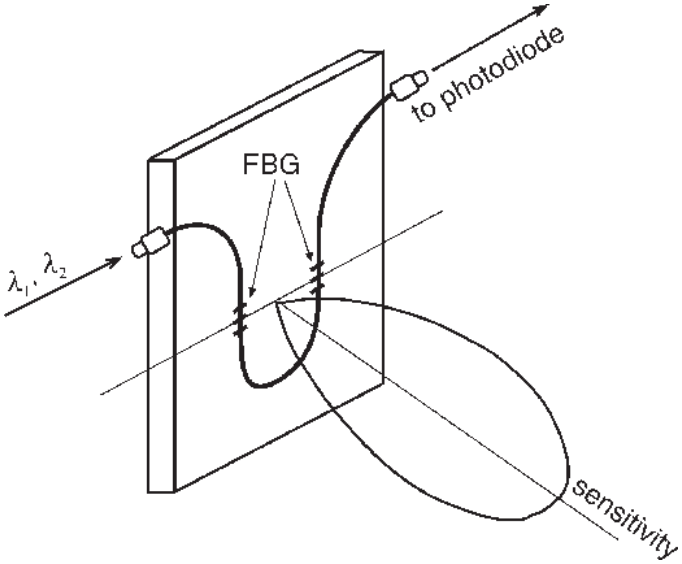

Figure 2. FBG hydrophone with directional sensitivity.

The hydrophone was examined in the acoustic frequency range from 1kHz to 3.2MHz and found to work well: the sensitivity was nearly constant. The lowest sound pressure that we measured with the hydrophone in Figure 1 was about 80dB for 1mPa at 20kHz. This is not considered to be a lower limit because the sensor has not yet been optimized and development is still in progress. The dynamic range of the measured sound pressure was about 90dB. The strongest sound pressure measured is not limited by the performance of the FBG hydrophone but by the ability to produce large acoustic fields in water with our laboratory equipment.

Figure 2 shows an FBG hydrophone head that has directional sensitivity. Two FBGs are in a single fiber and have different Bragg-reflection wavelengths. For sensor operation we need to prepare two narrow-spectrum light sources whose wavelengths are adjusted in the similar way to the hydrophone in Figure 1. Each beam is intensity-modulated by its own FBG and the transmitted light is detected by a photodiode. Specifically, the photocurrents produced in the photodiode by the two optical wavelengths are added together in the photodiode, resulting in the directional dependence of the sensor sensitivity as shown in Figure 2.

Nobuaki Takahashi
Department of Communications Engineering
National Defense Academy
1-10-20 Hashirimizu
Yokosuka, Kanagawa 239-8686
Japan
E-mail: tak@nda.ac.jp

References

1. P. J. Nash, J. Latchem, G. Cranch, S. Motley, A. Bautista, C. Kirkendall, A. Dandridge, M. Henshaw, and J. Churchill, *Design, Development and Construction of Fiber-Optic Bottom Mounted Array,* **Proc. 15th Optical Fiber Sensors Conference,** p. 333, 6 May 2002.
2. N. Takahashi, K. Yoshimura, S. Takahashi, and K. Imamura, *Development of an optical fiber hydrophone with fiber Bragg grating,* **Ultrasonics 38**, p. 581, March 2000.
3. N. Takahashi, K. Yoshimura, S. Takahashi, and K. Imamura, *Characteristics of fiber Bragg grating hydrophone,* **IEICE Trans. Electron. E83-C,** p. 275, March 2000.

Attractive potential for donor and acceptor states in photonic crystals with defects

Using the $\mathbf{k} \cdot \mathbf{p}$ theory to study photons in a photonic crystal with defects, we have found that the incident photon excites a quasi particle (QP) of photons from the periodic background field. This QP contains an inertial mass due to an energy-storing mechanism in the photonic crystals. We found the trapping of the QP is similar to quantum mechanics, in that an attractive potential formed at the defect that is linearly proportional to the product of the inertial mass and the normalized dielectric constant in a way that cannot be explained by microcavity theory.

If a small defect is introduced in the photonic crystal, it is possible to create highly-localized defect modes of the EM wave inside the gap. These defect modes are analogous to the localized impurity states in a semiconductor.[1] From special relativity, a moving particle with inertia always has a rest frame. However, there is no rest frame for the massless photon, since it moves with the velocity of light c in every frame of reference.[2] It is obvious, then, that a defect can stop and trap a particle with inertia, but not massless photons. We will explain the trapping effect of defects in a photonic crystal by proving that the equation of motion of the envelope function indeed includes an inertial-mass dependent trap potential.

We start from the Hermitian equation of magnetic field $H(r)$ for studying the photonic crystal:

$$\nabla \times [\frac{1}{\in(\mathbf{r})}(1+V(\mathbf{r}))\nabla \times \mathbf{H}(\mathbf{r})] = \frac{\omega^2}{c^2}\mathbf{H}(\mathbf{r}),$$

where $\varepsilon(r)$ is the periodic dielectric constant and $V(r)$ is the normalized defect dielectric disorder. By expanding $H(r)$ in terms of Kohn-Luttinger function, we can define the reciprocal effective-dielectric tensor[3,4] near the band edge as in Reference 5. By following the derivation of de Sterke and Sipe,[6] we obtain a time-dependent equation of the envelope function $F_n(r,t)$:

$$\frac{(i\hbar)^2}{c^2}\frac{\partial^2}{\partial t^2}F_n(\mathbf{r},t) = [(m_n c)^2 - \sum_{\alpha\beta}\left|\frac{\hbar^2}{\in_n^*}\right|_{\alpha\beta}\frac{\partial}{\partial x^\alpha \partial x^\beta} + U(\mathbf{r})]F_n(\mathbf{r},t)$$

This equation is the evolution equation of the EM-wave envelope function under the $\mathbf{k} \cdot \mathbf{p}$ theory, which is the generalized Klein-Gordon equation and which reduces to the Klein-Gordon equation[7] in an isotropic medium. It indicates that there is an energy-storing mechanism near the band edges.[8]

Here we have defined $m_n = \hbar\,\omega_n(k_0)/c^2$ as the inertial mass of a quasi-particle of photons. Here k is a wave vector that lies within the first Brillouin zone and k_0 is a specific wave-vector at the band maximum or minimum. The inertial mass m_n depends on the band index n and is quantized, and $U(r) = \pm(m_n c)^2 V(r)$ with the plus (or minus) sign given for the air-band (or the dielectric-band) QP. $U(r)$ is a potential produced by the defect and is negative as an attractive potential for the air-band QP with a dielectric defect. It is an attractive potential for an air defect in the dielectric band QP with $V(r)>0$. There is no attractive potential $(U(r)=0)$, when the inertial mass of a QP is zero $(m_n=0)$. Therefore, from the existence of an inertial mass, a QP of Bloch photons can be trapped by an arbitrarily weak attractive potential in one dimension, but not in three.

Summary

That the QP possesses inertia successfully explains not only the trapping effect of defects in a way analogous to quantum mechanics, but also explains the dielectric and air defects production of donor and acceptor states in the photonic band gap (PBG). The trapping effect of defects in PBG is similar to that in quantum mechanics in that an arbitrarily weak attractive potential can bind a state in one dimension, but not in three. These phenomena cannot be explained by the microcavity theory because it has no attractive trapping potential when the inertial mass of a QP is zero $(m_n=0)$.

The work was partially supported by the National Science Council of Republic of China under grant No. NSC-90-2112-M-009-050 and NSC-90-2112-M-034-004.

Szu-Cheng Cheng* and Wen-Feng Hsieh†
*Department of Physics
Chinese Culture University
Yang Ming Shan
Taipei 114, Taiwan
†Institute of Electro-Optical Engineering
National Chiao Tung University
1001, Tahsueh Rd.
Hsin Chu 300, Taiwan
E-mail: wfhsieh@cc.nctu.edu.tw

References

1. E. Yablonovitch et al., *Donor and acceptor modes in photonic band structure,* **Phys. Rev. Lett. 67,** p. 3380, 1991.
2. V. B. Berestetskii, E. M. Lifshitz, and L. P. Pitaevskii, **Quantum Electrodynamics,** 2nd edition., Pergamon Press Inc., New York, p. 25 1979.
3. N. F. Johnson and P. M. Hui, *Theory of propagation of scalar waves in periodic and disordered composite structures,* **Phys. Rev. B 48,** p. 10118, 1993.
4. N. F. Johnson, P. M. Hui, and K. H. Luk, *Theory of photonic band structures: a vector-wave approach,* **Solid State Commun. 90,** pp. 229, 1994.
5. J. E. Sipe, *Vector approach for photonic band structures,* **Phys. Rev. E 62,** p. 5672, 2000.
6. C. Martijn de Sterke and J. E. Sipe, *Extensions and generalizations of an envelope-function approach for the electrodynamics of nonlinear periodic structures,* **Phys. Rev. A 39,** p. 5163, 1999.
7. C. Itzykson and J. B. Zuber, **Quantum Field Theory,** McGraw-Hill Inc., 1980.
8. M. Scalora et al., *Ultrashort pulse propagation at the photonic band edge: Large tunable group delay with minimal distortion and loss,* **Phys. Rev. E 54,** p. 1078, 1996.

Tell us about your news, ideas, and events!

If you're interested in sending in an article for the newsletter, have ideas for future issues, or would like to publicize an event that is coming up, we'd like to hear from you. Contact our technical editor, Sunny Bains (sunny@spie.org) to let her know what you have in mind and she'll work with you to get something ready for publication.

Deadline for the next edition, 14.2, is:

28 March 2003: Suggestions for special issues and guest editors.

14 April 2003: Ideas for articles you'd like to write (or read).

16 June 2003: Calendar items for the twelve months starting January 2003.

A photorefractive polymer for 3D bit optical data storage and micro-fabrication

The requirement for increasing information storage capacity has been the driving force behind several new and innovative methods. The two main directions that this research has taken focus on reducing the size of the information bits stored in a single layer, and recording multiple layers/pages in order to use the recording medium's volume. Three-dimensional bit optical storage falls under the second category, whereby multiple layers are recorded through the depth of the recording medium. In this article we report on our recent development of rewritable 3D bit optical data storage and the formation of micro-voids in a photorefractive polymer.

Photorefractive polymer is a promising material for optical data storage and other photonic applications. We recently reported on the photorefractive effect under two-photon excitation in a photorefractive polymer,[1] which should make possible the developement of a low-cost, rewritable, 3D optical storage system (see example in Figure 1). The used photorefractive polymer consists of 2,5-dimethyl-4-(*p*-nirtophenylazo)anisole (DMNPAA), 2,4,7-trinitro-9-fluorenone (TNF), 9-ethylcarb-azole and poly(*N*-vinylcarbazole) (PVK).

To record multiple layers within a homogeneous medium, a nonlinear interaction between the recording laser beam and the material needs to take place. This was achieved using two-photon excitation; whereby the region of excitation depended quadratically on the intensity of the incident light. Typically, an ultrashort laser pulse is used because the cooperative nature of two-photon excitation requires the use of a high-peak-power laser to produce efficient excitation.This increases the cost of the recording device and makes it difficult to produce a compact system.

We demonstrated that the use of continuous-wave illumination for two-photon excitation was possible in a poly(Methyl Methacrylate) (PMMA) based photorefractive polymer.[2] Figure 2 shows the writing, erasing and rewriting of information into the same region of the photorefractive polymer. Figure 2(b) shows the same region as seen in Figure 2(a) including a recorded pattern (the letter E), after being exposed to the ultra-violet illumination for 1-2s. The result is the complete erasure of the previously recorded information. In Figure 2(c), a new pattern (the letter F) is written into the same area used in Figures 2(a) and (b). Two artifacts (marked 1 and 2 in Figures 2(a-c)) show that the same area was used in each case.

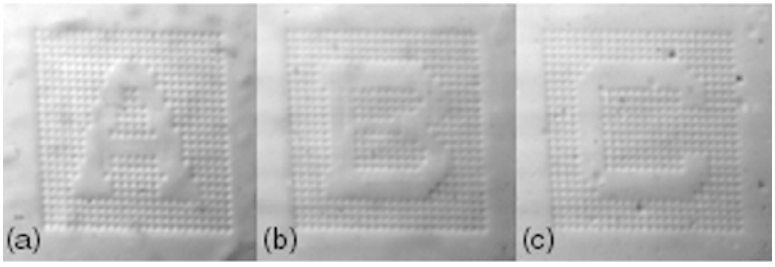

Figure 1. Recorded 24×24 bit patterns at different depths in the photorefractive polymer using two-photon excitation. The spacing between adjacent layers is 20μm, and the bit separation is 3.2μm. (a-c) The first, second and third layers including the letters 'A', 'B', and 'C', respectively.

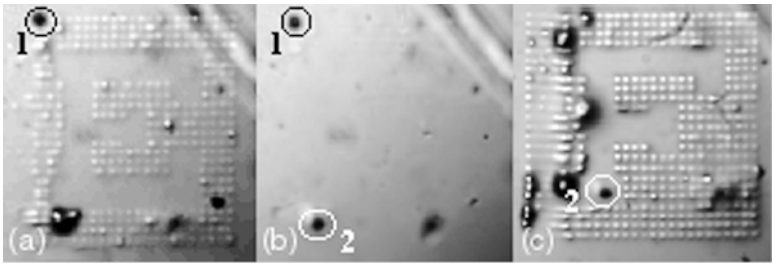

Figure 2. Demonstration of writing, erasing, and rewriting in an area under continuous-wave illumination with power 75mW and wavelength 800nm. (a) Letter 'E' is recorded. (b) Letter 'E' is erased after being exposed to UV illumination for 1-2s. (c) Letter 'F' is recorded in the same area.

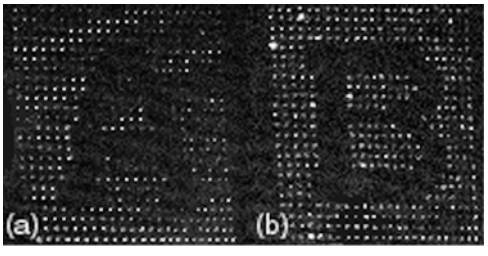

Figure 3. Multi-layered arrays of voids in a third type of PMMA-based photorefractive polymer. (a) The first layer, including the letter 'A', is recorded near the surface. (b) The second layer, including the letter 'B', is recorded 15μm deeper than the first. The images are readout by confocal reflection microscopy.

Another advantage of the PMMA-based photorefractive polymer is that the transition region from the erasable nature to the optical damage point is short. Thus it is a good candidate for fabricating microstructures under multi-photon excitation. We have observed the formation of voids in the PMMA-based photorefractive polymer according to the micro-explosion mechanism.[3] One of the applications of the voids is in read-only 3D bit optical data storage, as shown in Figure 3. If the laser beam used for forming a void is scanned at an appropriate speed, a microstructure can be created.

We have extended the traditional role of photorefractive materials to encompass a new range of photonic applications. Further research is likely to include the formation of complex 3D waveguides and photonic bandgap structures.

The authors would like to acknowledge the support from the Australian Research Council.

Daniel Day and Min Gu
Centre for Micro-Photonics
School of Biophysical Sciences and Electrical Engineering
Swinburne University of Technology
PO Box 218, Hawthorn
Victoria 3122, Australia
E-mail: dday@groupwise.swin.edu.au

References

1. D. Day, Min Gu, and A. Smallridge, *Use of two-photon excitation for erasable/rewritable three-dimensional bit optical data storage in a photorefractive polymer*, **Opt. Lett. 24**, p. 948, 1999.
2. D. Day, Min Gu, and A. Smallridge, *Rewritable three-dimensional bit optical data storage in a PMMA-based photorefractive polymers with continuous wave illumination*, **Advanced Materials 13**, p. 1005, 2001.
3. D. Day and M. Gu, *Formation of voids in a doped polymethylmethacrylate polymer*, **App. Phys. Lett. 80**, p. 2404, 2002.

Optically-interconnected computing at Heriot-Watt University

Continued from cover.

layer for their corresponding PC and transferred to them as required. If a SPA starts to run out of work, it randomly collects tasks from other SPAs. By implementing this at the optical-highway level, the large amount of network traffic created by this, often speculative, transfer of jobs is independent of the processing system's I/O bus.

In our group's second project, NOSC (Neural Optoelectronic Switch Controller), an optoelectronic neural network was constructed using optics to perform interconnection and off-the-shelf-electronics to provide neuron functionality. Although it is relatively simple to connect two people via a switch, real systems must accommodate many connections simultaneously: even under adverse conditions such as localized overloading or hardware failure. Neural networks have the ability to solve such scheduling problems efficiently, but limitations to the complexity and scalability of electrical interconnects on a conventional silicon chip have so far hindered the construction of any hardware.

In the system, arrays of detectors and VCSELs act as neuron inputs and outputs with complex neural interconnection patterns woven through free-space using a single diffractive optical element. Neural summation is simply the amount of light incident on a neuron's detector. All that electronics need do is choose the neuron's next response based on input light and communicate with the outside world. The first generation demonstrator,[2] constructed in collaboration with BT, took up the majority of an optical bench. The recently completed second generation demonstrator pushed integration and functionality further: the hardware now fits into a shoe-box. The third generation, currently at the concept stage, is intended to fully integrate the commodity components currently used onto a single chip. This level of integration is approaching that required for commercial viability.

The adaptation and optimization of algorithms for the specific hardware used, has considerably increased system scalability and performance. Indeed, doubling the size of the packet-switch routing problem only increases the time required to reach a solution by a couple of percent. Since the range of problems that a neural network can solve is vast, minimal alteration allows adaptation to a variety of tasks. These range from image recognition to general optimization and task allocation problems.

Heriot-Watt's OIC Group is now starting on two new projects. One, a European Union funded project, is to construct—with a number of collaborators—an optically-interconnected processor-memory bus for a multi-processor machine. The second is to integrate optical interconnects with reconfigurable silicon electronics in the form of Field Programmable Gate Arrays (FPGAs). Both of these will build on the successes of the previous projects.

Gordon A. Russell, K. J. Symington, and J. F. Snowdon
Department of Physics
Heriot-Watt University
Edinburgh, Scotland, UK
E-mail: g.a.russell@hw.ac.uk
http://www.optical-computing.co.uk

References

1. B. Layet and J. F. Snowdon. *Comparison Of Two Approaches For Implementing Free-Space Optical Interconnection Networks*. **Optics Communications 189,** pp. 39-46, March 2001.
2. R. P. Webb, A. J. Waddie, K. J. Symington, M. R. Taghizadeh, and J. F. Snowdon, *An Optoelectronic Neural Network Scheduler for Packet Switches*, **Applied Optics 39** (5), pp. 788-795, February 2000.

All-optical pulse generators for optical computing

Continued from page 3.

of first-pulse processing techniques from neural-network-modelling research shows that there are significant and meaningful computations that can be done with fully-parallel, pulse-based algorithms.

John L. Johnson
Science Advisor
US Army V Corps
E-mail: science@hq.c5.army.mil

References

1. R. Wang, P. Yeh, H.-C. Chang, X. Yi, and J. Zhao, *All-optical pulse generators for pulse-coupled neurons,* **Proc. SPIE 3715,** p. 46, 1999.
2. S. J. Thorpe, A. Delorme, and R. Van Rullen, *Spike-based strategies for rapid processing,* **Neural Networks 14** (6-7), p. 715, 2001.
3. A. Delorme and S. J. Thorpe, *Face identification using one spike per neuron: resistance to image degradations,* **Neural Networks 14** (6-7), p. 795, 2001.

Detection of 3D object position

Continued from page 2.

coordinate system of each elemental image to polar coordinates about the center of the elemental image. This increases discrimination ability.

Figure 2 shows an overall flow-chart of the proposed method. Each elemental image is transformed to polar coordinates and the *r*-coordinate is changed to ln(*r*) for the Mellin transform. The *f*-coordinate needs not be changed since the *f*-coordinate is not dependent on the size of the image. Each elemental image of the reference object is then correlated with the set of the elemental images of the signal object by JTC. The 3D position of the signal object relative to the reference object can be found by detecting the elemental image pair at angle zero that produces the highest correlation peak. The lateral shift represents the lateral spacing between two elemental lenses at angle zero, and the longitudinal shift can be found by the size difference of the perspective, calculated from the position of the correlation peak with respect to the center of the corresponding elemental image.

This approach can be improved further by non-uniformly placing the entire set of elemental images of the reference and signal objects in the input plane of the JTC simultaneously. This decreases processing time since correlations between all the pairs of elemental images are obtained at once.

Jae-Hyeung Park, Sungyong Jung, Heejin Choi, and Byoungho Lee
National Research Laboratory
for Holography Technologies
School of Electrical Engineering
Seoul National University
Shinlim-Dong, Kwanak-Gu,
Seoul 151-744, Korea
Tel: +82 2 880-7245
Fax: +82 2 873-9953
E-mail: byoungho@plaza.snu.ac.kr

References

1. J. Rosen, *Three-dimensional optical Fourier transform and correlation,* **Opt. Lett. 22,** p. 964-966, 1997.
2. B. Javidi and E. Tajahuerce, *Three-dimensional object recognition by use of digital holography,* **Opt. Lett. 25,** p. 610-612, 2000.
3. O. Matoba, E. Tajahuerce, and B. Javidi, *Real-time three-dimensional object recognition with multiple perspectives imaging,* **Appl. Opt. 40,** p. 3318-3325, 2001.
4. J.-H. Park, S. Jung, S.-W. Min, and B. Lee, *Detection of longitudinal or lateral shift in three-dimensional correlator using a lens array,* **Int'l Conf. on Optics in Computing**, Taipei, Taiwan, pp. 57-59, April 2002.

Femtosecond optical information processing

Continued from page 5.

Photonics Technology Letters 11, p. 827, 1999.
5. S. Shen, A. M. Weiner, and G. D. Sucha, *Bit Error Rate Performance of Ultrashort-Pulse Optical CDMA Detection Under Multi-Access Interference*, **Electronics Letters 36,** p. 1795, 2000.
6. D. E. Leaird and A. M. Weiner, *Femtosecond Direct Space-to-Time Pulse Shaping*, **IEEE J. Quantum Electron. 37,** p. 494, 2001.
7. D. E. Leaird, A. M. Weiner, S. Kamei, M. Ishii, A. Sugita, and K. Okamoto, *Generation of flat-topped 500-GHz pulse bursts using loss-engineered arrayed waveguide gratings*, **IEEE Phot. Tech. Lett. 14,** p. 816, 2002.
8. P. C. Sun, Y. T. Mazurenko, and Y. Fainman, *Femtosecond Pulse Imaging: Ultrafast Optical Oscilloscope*, **J. Opt. Soc. Am. A 14,** p. 1159, 1997.
9. Ayman M. Kanan and A. M. Weiner, *Efficient time-to-space conversion of femtosecond optical pulses*, **J. Opt. Soc. Am. B 15,** p. 1242, 1998.
10. J.-H. Chung and A. M. Weiner, in preparation.
11. Z. Zheng and A. M. Weiner, *Spectral phase correlation of coded femtosecond pulses by second-harmonic generation in thick nonlinear crystals*, **Opt. Lett. 25,** p. 984, 2000.
12. Z. Zheng, A. M. Weiner, K. R. Parameswaran, M. H. Chou, and M. M. Fejer, *Low Power Spectral Phase Correlator Using Periodically Poled $LiNbO_3$ Waveguides*, **IEEE Phot. Tech. Lett. 13,** p. 376, 2001.

Information extraction from amino-acid sequences using a spatially-coded moiré matching technique

Continued from page 12.

requirement using hydropathy and classification coding to extract similarities between sequences. Figure 2(a) shows the classification coding rule[4] where 20 amino elements are classified into four groups according to side-chain characteristics: nonpolar, polar, acidic , and basic. Four code patterns are assigned to the individual groups.

Figure 2(b) shows the matching result. The positions of the broken and shifted segments in Figure 2(b) match the positions of deletion or insertion obtained by CLASTAL W, a popular alignment tool. Figure 2(b) indicates that SCMM is effective for extracting similarity, with ambiguity, between amino-acid sequences using the new coding rule. These features are expected to be useful for extracting weak sequence similarities, such as motifs,[4] and to detect homology overlooked by current genome-analysis tools.

Kouichi Nitta* and Jun Tanida†
*Department of Material and Life Science
Graduate School of Engineering
†Department of Information and Physical Sciences
Graduate School of Information Technology and Science
*†Osaka University
2-1 Yamadaoka Suita 565-0871, Japan.
E-mail: {nitta@photonics.mls.eng, tanida@ist}.osaka-u.ac.jp

References

1. J. Tanida**, Opt. Lett. 24,** pp. 1681-1683, 1999.
2. K. Nitta, H. Togo, and J. Tanida, **Opt. Eng. 40,** pp. 2386-2391, 2001.
3. K. Nitta, A. Yahata, and J. Tanida, **Proc. Optics in Computing 2002,** pp. 65-67, 2002.
4. A. Gibbs and G. McIntyre, **Eur. J. Biochem. 16,** pp.1-11, 1970.

CALENDAR

2002

SPIE's Photonics Fabrication
28 October–1 November
Brugge, Belgium
Program
http://spie.org/conferences/calls/02/epf/

ATOM02

Advanced Topics in Optoelectronics: Micro- and Nanotechnology
21–23 November
Bucharest, Romania
SPIE will publish Proceedings. Sponsored by: SPIE - RO Chapter, National Institute for Physics Matter (INFM) Italy, Romanian Ministry of Education and Research, IEEE - Romanian Section
Program
http://joe.tehfi.pub.ro/atom2002.htm

International Symposium on Smart Materials, Nano- and Micro-Smart Systems
16–18 December
Melbourne, Australia
Note: Dates have changed to 16–18 December and abstract due date was extended.
Call for Papers. Abstracts Due 15 July 2002
http://spie.org/conferences/calls/02/au

For More Information Contact
SPIE • PO Box 10, Bellingham, WA 98227-0010
Tel: +1 360 676 3290 • Fax: +1 360 647 1445 • E-mail: spie@spie.org • Web: www.spie.org

2003

Electronic Imaging 2003
20–24 January
Santa Clara, California USA
Call for Papers. Abstracts Due 24 June 2002
Exhibition
http://electronicimaging.org/call/03

Photonics West
25–31 January
San Jose, California USA
Call for Papers. Abstracts Due 1 July 2002
Exhibition
http://spie.org/conferences/calls/03/pw/

The International Symposium on Optical Science and Technology

SPIE's 48th Annual Meeting
3–8 August
San Diego, California USA
Exhibition
http://spie.org/app/exhibition/index.cfm

Join the Technical Group

...and receive this newsletter

Membership Application

Please Print ☐ Prof. ☐ Dr. ☐ Mr. ☐ Miss ☐ Mrs. ☐ Ms.

First Name, Middle Initial, Last Name _____

Position _____ SPIE Member Number _____

Business Affiliation _____

Dept./Bldg./Mail Stop/etc. _____

Street Address or P.O. Box _____

City/State _____ Zip/Postal Code _____ Country _____

Telephone _____ Telefax _____

E-mail Address/Network _____

Technical Group Membership fee is $30/year, or $15/year for full SPIE members.

❑ Optics in Information Systems
Total amount enclosed for Technical Group membership **$** _____

❑ **Check enclosed.** Payment in U.S. dollars (by draft on a U.S. bank, or international money order) is required. Do not send currency. Transfers from banks must include a copy of the transfer order.

❑ **Charge to my:** ❑ VISA ❑ MasterCard ❑ American Express ❑ Diners Club ❑ Discover

Account # _____ Expiration date _____

Signature _____
(required for credit card orders)

This newsletter is printed as a benefit of the **Optics in Information Systems Technical Group.** Membership allows you to communicate and network with colleagues worldwide.

As well as a semi-annual copy of the *Optics in Information Systems* newsletter, benefits include SPIE's monthly publication, *oemagazine*, and a membership directory.

SPIE members are invited to join for the reduced fee of $15. If you are not a member of SPIE, the annual membership fee of $30 will cover all technical group membership services. For complete information and an application form, contact SPIE.

Send this form (or photocopy) to:
SPIE • P.O. Box 10
Bellingham, WA 98227-0010 USA
Tel: +1 360 676 3290
Fax: +1 360 647 1445
E-mail: spie@spie.org

http://www.spie.org/info/ois

Please send me
☐ Information about full SPIE membership
☐ Information about other SPIE technical groups
☐ FREE technical publications catalog

Reference Code: 3152

OPTICSONLINE

Optics Web Discussion Forum

You are invited to participate in SPIE's online discussion forum on *Optics in Information Systems*.

You'll find our forums well-designed and easy to use, with many helpful features such as automated email notifications, easy-to-follow 'threads,' and searchability. There is also a full FAQ for more details on how to use the forums.

To post a message, log in to create a user account. For options see the "subscribe to this forum" page.

Main link to the *Optics in Information Systems* forum:

`http://spie.org/app/forums/tech/`

Related questions or suggestions can be sent to `forums@spie.org`.

SPIE The International Society for Optical Engineering

Optics in Information Systems

This newsletter is published semi-annually by SPIE—The International Society for Optical Engineering, for its International Technical Group on Optics in Information Systems.

Editor and Technical Group Chairs Bahram Javidi, Demetri Psaltis
Technical Editor Sunny Bains
Managing Editor Linda DeLano
Advertising Sales Gayle Lemieux

Articles in this newsletter do not necessarily constitute endorsement or the opinions of the editors or SPIE. Advertising and copy are subject to acceptance by the editors.

SPIE is an international technical society dedicated to advancing engineering, scientific, and commercial applications of optical, photonic, imaging, electronic, and optoelectronic technologies. Its members are engineers, scientists, and users interested in the development and reduction to practice of these technologies. SPIE provides the means for communicating new developments and applications information to the engineering, scientific, and user communities through its publications, symposia, education programs, and online electronic information services.

SPIE—The International Society for Optical Engineering, P.O. Box 10, Bellingham, WA 98227-0010 USA. Tel: +1 360 676 3290. Fax: +1 360 647 1445.

European Office: Karin Burger, Manager, karin@spieeurope.org, Tel: +44 7974 214542. Fax: +44 29 2040 4873.

In Japan: c/o O.T.O. Research Corp., Takeuchi Bldg. 1-34-12 Takatanobaba, Shinjuku-ku, Tokyo 160, Japan. Tel: +81 3 3208 7821. Fax: +81 3 3200 2889. E-mail: otoresco@gol.com

In Russia/FSU: 12, Mokhovaja str., 121019, Moscow, Russia. Tel/Fax: +7 95 202 1079. E-mail: edmund@spierus.relcom.ru

Information extraction from amino-acid sequences using a spatially-coded moiré matching technique

Optical computing techniques are expected to be useful for large-scale information processing by exploiting features of light such as large parallelism, huge information capacity, excellent visualization capability, and so on. However, relatively few of these techniques have been used in practical applications. It has been pointed out that when suitable applications of optical computing have been properly demonstrated, the situation within the field will improve.[1] Spatially-coded moiré matching (SCMM), a method of matching strings, should prove useful in genome sequence analysis and, thus, is expected to be a practical technique based on optical computing.

Figure 1(a) shows the SCMM processing procedure.[1] First, images of the target strings S_1 and S_2 are built up: each composed of patterns obtained in accordance with the coding rule. Figure 1(b) depicts the rule assigning each of the DNA bases—A, G, C, and T—to a spatial code pattern. Moiré fringes are obtained by overlapping two coded images with a small intersection angle.

The output moiré patterns provide the result of the matching operation for multiple combinations, with different amounts of relative shift between the sequences, in parallel. The patterns contain useful information, allowing the extraction of function, the prediction of the evolutionary relationships between species, and so on. Bright segments in the moiré fringes appear at positions where both target elements are identical. Deletion and insertion between sequences are extracted as discontinued segments. Reiterated sequences are obtained as short segments aligned vertically.[2]

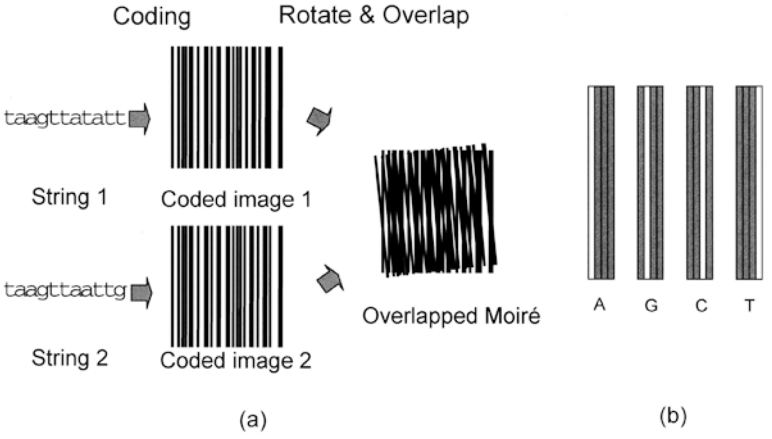

Figure 1. (a) SCMM processing procedure. (b) Code patterns for DNA bases.

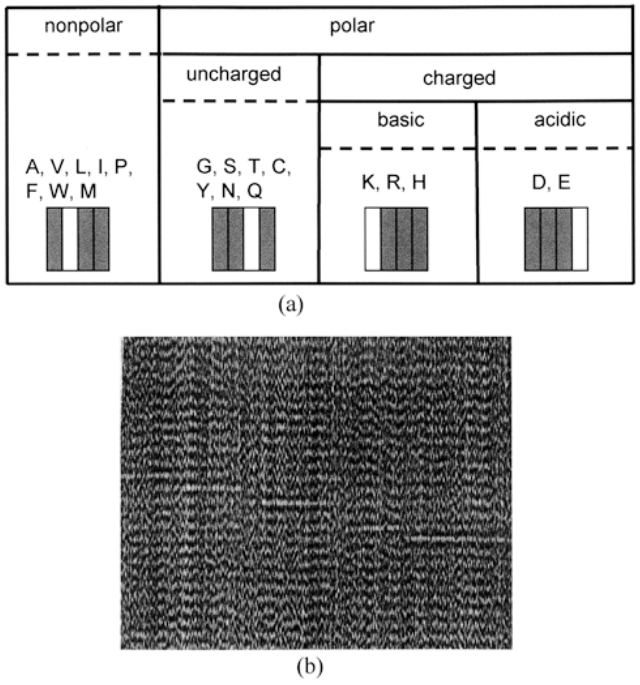

Figure 2. (a) The classification coding rule. (b) Amino sequence matching using the classification coding rule.

Although the SCMM technique provides outputs similar to the dot matrix method,[3] the former has various advantages.[2] Though the dot matrix is one of the fundamental methods for sequence comparison, and is widely used in genome analysis, the SCMM has a visualization capability that comes from its optical nature. We have constructed the prototype matching-information terminal based on the SCMM.[2] With the help of a personal-computer-controlled display, the terminal allows dynamic change in the target strings, easy access to genome databases, and other features useful for genome sequence analysis.

The SCMM technique can be extended to amino-acid sequence comparison by a specific coding rule. Amino-acid sequence matching is different from DNA sequencing, because amino-acid elements cannot be dealt with as simple letters. This is because, in amino-acid sequencing, the chemical characteristics of the amino acids are important in order to determine the structure and the function of the protein. Also, amino sequences with weak similarity often construct highly similar structures and have common functions. Therefore, a matching operation permitting some ambiguity is required for amino-acid sequence analysis.

The SCMM can satisfy this

Continues on page 11.

SPIE Society of Photo-Optical Instrumentation Engineers

P.O. Box 10 • Bellingham, WA 98227-0010 USA

Change Service Requested

DATED MATERIAL

Non-Profit Org.
U.S. Postage Paid
Society of
Photo-Optical
Instrumentation
Engineers